INVESTIGATING ACOUSTIC PROPAGATION IN GASSY MARINE SEDIMENTS USING A BUBBLY GEL MIMIC

Gary B.N. Robb[a], Timothy G. Leighton[b], Victor F. Humphrey[b], Angus I. Best[a], Justin K. Dix[a] and Zygmunt Klusek[c]

[a]National Oceanography Centre, Southampton, University of Southampton, Waterfront Campus, European Way, Southampton, SO14 3ZH, U.K.
[b]Institute of Sound and Vibration Research, University of Southampton, Southampton, SO17 1BJ, U.K.
[c]Institute of Oceanography, Polish Academy of Sciences, Sopot, P.O. Box 148, Poland.

Corresponding author: Gary B.N. Robb, National Oceanography Centre, Southampton, University of Southampton, Waterfront Campus, European Way, Southampton, SO14 3ZH, U.K. (fax: +44 2380 596667; email: gbor199@noc.soton.ac.uk)

Abstract: *The acoustic techniques available for the determination of bubble size distributions in fluids are presently more sophisticated than those available for gassy sediments. To provide a simplified platform for the testing of models for acoustic propagation in marine sediments, experiments have been performed on a bubbly gel mimic. This eliminates the granular and inhomogeneous nature of the host medium, while retaining its ability to support shear waves. Compressional wave velocities are measured in a bubbly xantham gel sample from 21 to 111 kHz. In the frequency range of 25 to 40 kHz, these display a sharp transition between the lower and upper asymptotic values of the velocity ratio. Bubble size distributions measured using CT scanning techniques possess modal radii from 70 to 110 µm, radii whose resonant frequencies directly correspond to the frequency range over which the sharp transition occurs. Velocity ratios predicted by the Anderson and Hampton acoustic theory for gassy sediments differ considerably from measured values, with predicted values very sensitive to the inclusion of bubbles with radii too small to be detected by the CT scanner, i.e. those bubbles having radii less than 20 µm.*

Keywords: *Bubbly media, acoustic propagation, xantham gel, CT scanning*

1. INTRODUCTION

Regions of seafloor sediments that contain gas bubbles, primarily methane, have been identified at numerous global locations [1]. These have been detected primarily through the significant impact of the bubbles on the bulk acoustic properties of the sediment, with typical "gassy" features observed on high-resolution seismic profiles including acoustic turbidity and blanking [2]. These features arise from the large and strongly frequency-dependent acoustic cross-section that each bubble presents to the insonifying sound field [3,4].

It would be beneficial to a number of marine applications if the existing acoustic capability to identify the spatial extent of gassy sediments could be extended to allow the bubble size distributions (BSDs) to be measured. First, the increased understanding of the acoustic properties of gassy sediments required to obtain measurements of BSDs from acoustic signals would greatly assist marine surveyors, possibly allowing the interpretation of previously disrupted regions on seismic profiles. Second, the bubble distribution will affect the shear strength and load-bearing capacity of the sediment [5,6] and will therefore be of interest to offshore geohazard assessment. Third, the flux of methane from the seabed to the atmosphere, of which climate modellers require more refined information [7], will depend on the BSDs present in the sediment.

The ability for a user to be able to determine BSDs quantitatively depends on the level of sophistication of both the acoustic measurement techniques and the acoustic theories available for inverting acoustic data obtained by these techniques. In comparison to water-based bubble populations, where non-linear, non-stationary acoustic theories have been developed [8-10], the existing theories for sediment-based bubble populations are limited to linear stationary scenarios [3,4]. Similarly, advanced acoustic measurement techniques, such as the analysis of non-linear sum and difference signals [9], are at a more advanced stage for water-based than sediment-based bubble populations.

While the more developed nature of the water-based measurements and theories can be partly attributed to their numerous industrial, medical and oceanographic applications [11], the uniform, homogeneous nature of the media containing the bubbles is also a factor. In contrast to the fundamental properties of water (e.g. velocity and density) which can be determined using standard predictive equations [12], the fundamental properties of the saturated sediment component of gassy sediments are difficult to predict. Recent work has identified that compressional wave velocities in sediments of the same sedimentological classification and depth, with similar porosities (variations of less than 1 %) and which are located within lateral distances of order 100 m can vary by up to 10 % [13], a value which agrees with previous research in this field [14]. In addition to this variability, which is attributed to the subtle differences in structure and grain size distribution of the sediment [13, 14], the ability of marine sediments to support shear forces adds a further level of complexity to the bubble host medium.

It would therefore be useful to investigate the acoustic properties of bubbly media in which the host media is homogeneous and supports shear, e.g. water-based gels. Therefore this paper presents a comparison of compressional wave velocities measured in bubbly xantham gel with those predicted by the sediment-based model of Anderson and Hampton [3,4], using bubble populations obtained through CT scanning techniques.

2. EXPERIMENT

Propagation experiments were performed on samples of xantham gel which were confined in a Polymethylmethacrylate (Perspex) box measuring 96 mm x 280 mm x 580 mm. This was suspended co-linearly along a horizontal axis with the required sources and receiver (as displayed in Fig. 1) in a large water tank, which measured 8 m x 8 m x 5 m deep. To span a wide frequency range two custom-made high-fidelity sources, developed by Neptune Sonar Ltd. and Blacknor Technology Ltd., were used. These included a low-frequency (LF) source which operates from 21 to 36 kHz and a high-frequency (HF) source which operates from 27 to 111 kHz. In order to achieve accurate positioning, all devices were deployed using purpose built carbon rods which were firmly attached to cross-bars across the top of the tank. The separation between the source and the sample (0.3 m) minimises beam spreading at the sample face (and therefore minimises the magnitude of diffractions and reflections from the box edges) while ensuring that the sample lies beyond the near-field to far-field transition of the sources (greater than 0.27 m for both sources). The position of the receiver also maximises the time difference between the diffraction and reflection events and the direct arrival, a factor which becomes more important at lower frequencies.

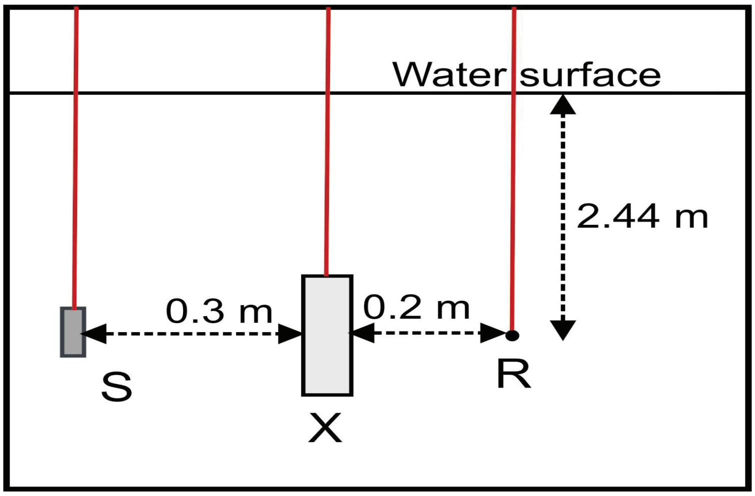

*Fig.1: Experimental setup, showing relative positions of source **S**, xantham sample **X** and receiver **R** at common depth of 2.44 m and separations of 0.3 m and 0.2 m respectively. All devices were deployed on carbon rods (denoted by vertical lines) to allow relative positions to be accurately obtained.*

A xantham gel, with a concentration by weight of 2 %, was selected as the host medium for the bubbles, owing to its ability to support bubble populations of a similar size to those observed in gassy sediments in nature, i.e. radii from 10s of μm to 10 mm (see review by Robb *et al.* [15]). As these populations remain stable over periods of the order of 2 to 4.5 hours for 0.8 % concentration gels [16], it is assumed that the bubbles present in the 2 % gel remain stable over the 6 hour period required to perform the acoustic measurements described here.

Initially bubble-free samples of the xantham gel were produced in a saline solution (35 ‰). The preparation of these samples at a water temperature of approximately 40 to 50 ^{o}C slowed the setting rate sufficiently to allow a homogeneous mixture of gel to form without the need for rapid stirring, a process which intrinsically introduces bubbles. Using the experimental arrangement in Fig. 1 the compressional wave group velocity of the bubble free gel was measured to be 1565 $m \cdot s^{-1} \pm 10\ m \cdot s^{-1}$, while the bulk density ρ of the bubble-free gel was independently measured to be 999 $kg \cdot m^{-3} \pm 10\ kg \cdot m^{-3}$. Additional portions of this gel were then whisked to introduce air bubbles with a wide range of sizes (radii from 10s of µm to cms). Bubbles with sizes broadly relevant to the frequency range under examination, i.e. radii of order 10s to 100s of µm, were then selected using a syringe with an aperture of order 200 µm and injected at discrete points into the bubble-free gel. The sample was then capped underwater to prevent the trapping of any large air voids. To obtain a measure of the BSD, three 5 ml sub-samples of bubbly gel were collected prior to the propagation experiments. These were immediately analysed using a X-Tek CT scanner, which uses the attenuation of X-rays to map the density composition of a material. The image resolution of each scan, which depends on the size of the sample and its position in the scanner, ranged from 12.1 to 12.8 µm for the three sub-samples examined.

Pulses containing three oscillations, with central frequencies ranging from 20 to 111 kHz in 1 kHz steps were generated using a D/A card with a 1 MHz sampling rate. These were transmitted through a matched power amplifier to the relevant source, with fifty shots acquired at each central frequency. Group velocities were obtained through the comparison of signals that had propagated through the bubbly gel sample with reference signals received without the sample present. Between these two sets of measurements the source and receiver were unmoved. In each case the received signals were stacked and filtered, using 3rd order Butterworth band-pass filters with pass-bands that scaled to account for the change in the bandwidth of the signals across the frequency band examined. Example reference (water-based) and sample signals are displayed in Fig. 2.

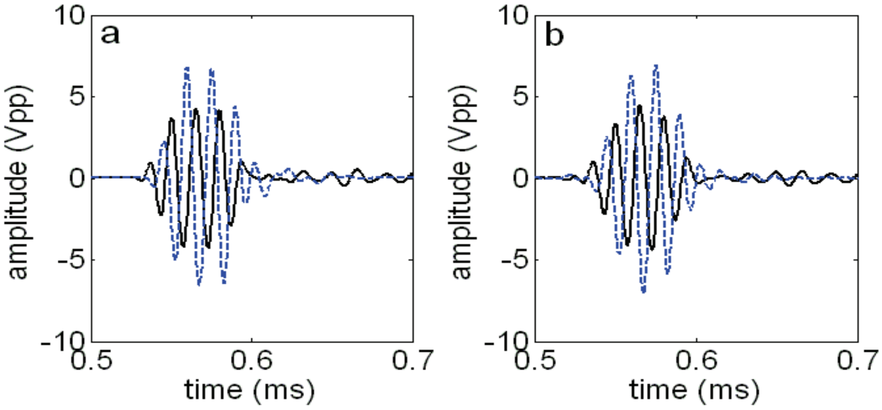

Fig.2: Example received signals at central frequency of 65 kHz, including a single, unprocessed signal (a) and the output of the processing stage (i.e. after the application of band-pass filtering and the stacking of 50 shots). Reference signals are displayed as dashed line, while the sample signals are displayed as solid lines

The time difference Δt between the sample signal and the reference signal was then determined from the maximum of the cross-correlation of the signal envelopes, with the envelopes computed using the Hilbert transform. The velocity v was calculated using:

$$v = \frac{d}{\left(\Delta t - t_C + d/v_W\right)} \qquad (1),$$

where d is the thickness of the sample and t_C is the time correction required to account for the insertion of the sample box (which introduces two 1 mm thick Perspex walls). Errors in the velocity, which range from 1.3 to 1.7 %, were obtained by propagating the timing resolution of the acquisition system (± 0.5 μs) and the uncertainties in the sample thickness (± 1 mm) through Equation 1.

3. RESULTS AND DISCUSSION

The measured velocity ratios (see Fig. 3) were obtained by dividing the measured group velocity by the velocity of the bubble-free gel. Velocity ratios appear to be relatively independent of frequency from 21 to 25 kHz and 40 to 111 kHz. A steep increase is observed in velocity ratio as frequency increases from 25 to 40 kHz with a strong agreement observed between the values determined from the two different sources.

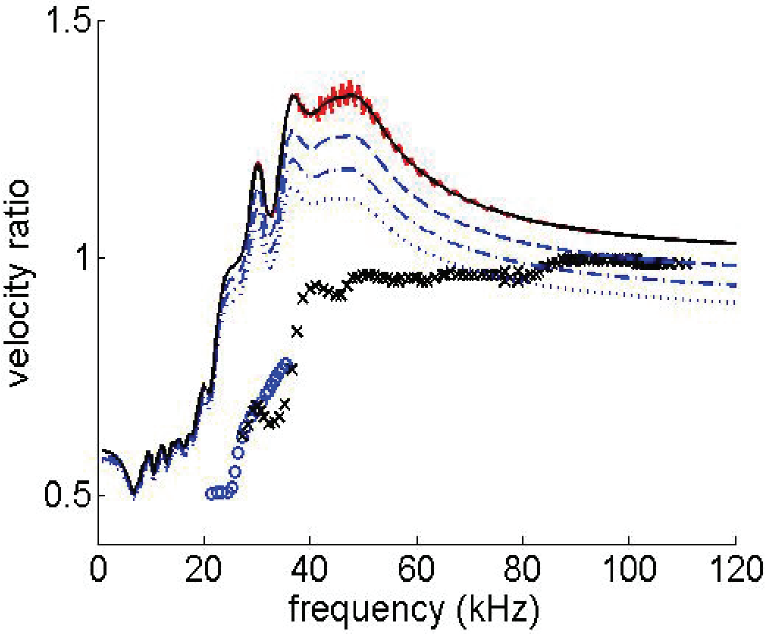

Fig.3: Measured and predicted velocity ratios. Measured velocity ratios are displayed for LF source (circles) and HF source (crosses). The predicted ratio of phase velocity in bubbly gel to that in bubble-free gel are shown for the best-fit population using 2.5 μm bins (oscillatory solid line) and 0.5 μm bins (smooth solid line). Predicted ratios are also shown for this best-fit population, using 0.5 μm bins, with additional Gaussian contributions added from 5 to 20 μm with void fractions of $1.7x10^{-3}$ (dash line), $3.5x10^{-3}$ (dotted line) and $5.1x10^{-3}$ % (dash-dot line).

The combined number of bubbles measured in the sub-samples (Fig. 4(a)) is dominated by radii r from 70 to 110 μm. The spherical nature of these bubbles is displayed in a 3-D volume from one of the samples (Fig. 4(b)). The resonant frequencies f_r of the modal radii were estimated, through the use of $f_r \cdot r = 3\ Hz \cdot m$ [11], to vary from 27 to 43 kHz. These values correspond well with the frequency range over which highly dispersive group velocities are measured. As the bubble population was observed to be strongly heterogeneous, the results of the CT scans can only be used to determine the BSD of the bulk sample. The void fraction was estimated to be 0.05 %, from the approximate volume of bubbles injected into the bubble-free sample. Note that no information could be obtained concerning bubbles with radii less than 30 μm, as these could not be detected above noise in the CT data.

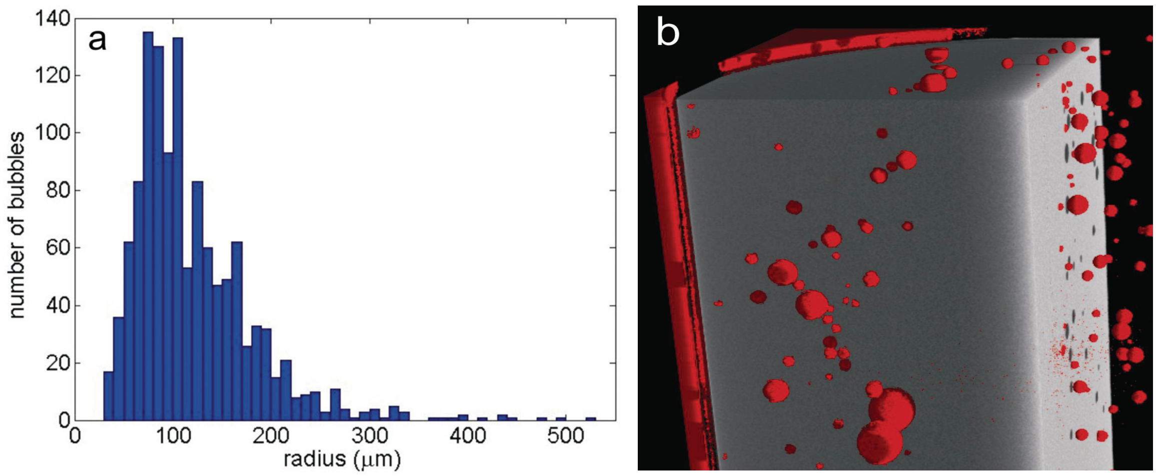

Fig.4: Measured bubble distribution, including: (a) combined bubble distribution obtained from the three sub-samples and (b) a 3-D CT image of a vertical segment of one of the cylindrical samples, with the host gel clipped back to allow the bubbles to be more clearly observed.

The acoustic theory of Anderson and Hampton [3,4] was used to predict the phase velocity of the bubbly gel. While this theory was developed for gassy marine sediments, through the incorporation of shear-based terms into the fluid-based theory of Silberman [17], it can be applied to any gassy medium in which the host medium possesses a finite shear modulus. The key parameters in this model are the BSD, which has been measured, and the bulk modulus K and shear modulus G of the host material.

A detailed examination of the extant literature revealed no values for the bulk and shear modulus of xantham gel at the frequencies of interest to this work. The shear modulus was therefore obtained by extrapolating shear moduli measurements made on xantham gel, at concentration of 4 %, from 160 mHz to 16 Hz [18]. These can be expressed in term of the frequency f using the following power law relationship:

$$G = 132 \cdot \left(f / f_o \right)^{0.152} \quad (2),$$

where f_o is 1 Hz. The extrapolation of this relationship to the kHz frequencies examined in this work produces an upper limit on the shear modulus of 800 Pa, which is three to four orders of magnitude less than the shear modulus of marine muds and five to six orders less than that of marine sands [19] at similar frequencies. The bulk modulus of the gel was then calculated using:

$$v = \sqrt{\frac{K + 4/3\, G}{\rho}} \quad (3).$$

As the bulk modulus of the gel will exceed that of water of a similar salinity and temperature, i.e. 2.3 GPa [12], it can be assumed that the shear modulus has a negligible effect in Equation 3 and can be omitted. The measured velocity (1565 $m \cdot s^{-1}$) and bulk density (999 $kg \cdot m^{-3}$) of the bubble-free gel give a bulk modulus of 2.45 GPa.

The measured bubble sizes were interpolated to 0.5 μm bins, as coarser bin size resulted in artefacts in the predicted (see Fig. 3). The void fraction was then adjusted to obtain a best-fit bubble population, with the resulting void fraction (0.013 %) approximately ¼ that of the estimated void fraction. This was achieved by fitting the upper and lower limits of the predicted phase velocity to corresponding plateaus in the measured group velocity There are however notable discrepancies between the predicted and measured values, in both the frequency range over which the transition from low to high velocity ratios occurs and the overall over-prediction of measured velocity ratios.

One possible explanation for the difference in the measured and predicted velocity ratios is that bubbles with radii less than 30 μm may be present. Tests indicated that the inclusion of additional Gaussian distributions which spanned radii from 5 to 20 μm acted to reduce the magnitude of the predicted velocity ratios from 20 to 80 kHz, without modifying the lower limit present at lower frequencies. Typical results are displayed in Fig. 3 for modified populations, which consist of the best-fit population, with a void fraction of 0.013 %, and additional Gaussian components from 5 to 20 μm with void fractions from 1.7×10^{-3} and 5.1×10^{-3} %.

Even with the inclusion of smaller unresolvable bubbles, the predicted velocity ratios differ considerably from the measured values. This may be a consequence of the comparison of predicted phase velocities with measured group velocities. These will differ for frequencies whose pulses possess bandwidth which extend into the measured range of dispersive velocities, namely pulses with central frequencies from 21 to 60 kHz. An alternative explanation is the linear nature of the model used, while the actual pressures that impinge on the sample are predicted to be 5 to 25 kPa (from known source levels, amplifier gains and beam patterns) and are likely to require the inclusion of non-linear effects [10].

4. CONCLUSIONS

The compressional wave velocity of a bubbly xantham gel sample was measured over the frequency range of 21 to 111 kHz. The velocity ratio between the bubbly gel and bubble-free gel displays a sharp transition between lower and upper asymptotes at frequencies between 25 to 40 kHz. The bubble size distribution measured using CT scanning techniques displays modal radii between 70 and 110 μm, the resonant frequencies of which directly correspond to the sharp transition in velocity ratio. The velocity ratios predicted by the acoustic theory of Anderson and Hampton [3,4] differ considerably from measured values. The inclusion of bubbles with radii less than 20 μm, i.e. those undetectable above the noise in the CT data, has a considerable effect on the predicted velocity ratios. The objectives of future work include the use of CT scanning to determine the long-term stability of bubble populations in the xantham samples and the measurement of the phase velocity, as described in [20], to allow direct comparison of measured and predicted velocity ratios.

5. ACKNOWLEDGEMENTS

This work has been funded by the Engineering and Physical Research Council (Grant No. EP/D000580/1; TG Leighton Principle Investigator). Thanks are extended to Paul Doust (Blacknor Technology Ltd., Portland, UK) for the development of the source amplifiers and to Professor Ian Sinclair (School of Engineering Sciences, University of Southampton) for permission to use the CT-scanner and assistance in doing so.

REFERENCES

[1] **P Fleischer, TH Orsi, MD Richardson** and **AL Anderson**, Distribution of free gas in marine sediments: a global overview, *Geo-Marine Letters*, **21**, pp. 103-122, 2001.

[2] **AG Judd** and **M Hovland**, The evidence of shallow gas in marine sediments, *Cont. Shelf Res.*, **12(10)**, pp. 1081-1095, 1992.

[3] **AL Anderson** and **LD Hampton**, Acoustics of gas bearing sediments I, Background, *J. Acous. Soc. of Am.*, **67**(6), pp. 1865-1889, 1980.

[4] **AL Anderson** and **LD Hampton**, Acoustics of gas bearing sediments II. Measurements and models, *J. Acous. Soc. of Am.*, **67**(6), pp. 1890-1903, 1980.

[5] **GC Sills, SJ Wheeler, SD Thomas** and **TN Gardiner**, Behaviour of offshore soils containing gas bubbles, *Geotechnique*, **41**(2), pp. 227-241, 1991.

[6] **SJ Wheeler** and **TN Gardiner**, Elastic moduli of soils containing large gas bubbles, *Geotechnique*, **39**(2), pp. 333-342, 1989.

[7] **AG Judd**, The global importance and context of methane escape from the seabed, *Geo-Marine Letters*, **23**, pp. 147-154, 2003.

[8] **TG Leighton**, Nonlinear Bubble Dynamics & The Effects On Propagation Through Near-Surface Bubble Layers, In *High-Frequency Ocean Acoustics*, MB Porter, M Siderius, & W Kuperman, American Institute of Physics, Melville, New York, pp. 180-193, 2005.

[9] **TG Leighton**, From babbling brooks to baby scans, from seas to surgeries: The pressure fields produced by non-interacting spherical bubbles at low & medium amplitudes of pulsation, *Int. J. of Modern Phys. B*, **18**(25), pp. 3267-3314, 2004.

[10] **TG Leighton, SD Meers** and **PR White**, Propagation through nonlinear time-dependent bubble clouds, & the estimation of bubble populations from measured acoustic characteristics. *Proc. of the Royal Soc. A*, **460**(2049), pp. 2521-2550, 2004.

[11] **TG Leighton**, *The Acoustic Bubble*, Academic Press, London, pp. 1-613, 1997.

[12] **P Siedler**, Properties of seawater, *Numerical data and functional relationships in science and technology*, Springer-Verlag, pp. 237-259, 1986.

[13] **GBN Robb, AI Best, JK Dix, JM Bull, TG Leighton** and **PR White**, The frequency-dependence of Compressional Wave Velocity and Attenuation Coefficient of Inter-tidal Marine Sediments, *J. Acous. Soc. of Am.*, **120**(5), pp. 2526-2537, 2006.

[14] **EL Hamilton**, Acoustic properties of sediments, In *Acoustics and the ocean bottom*, A Lara-Saenz, C Ranz-Guerra and C Carbo-Fite, CSIS Madrid, pp. 4-58, 1987.

[15] **GBN Robb, TG Leighton, JK Dix, AI Best, VH Humphrey** and **PR White**, Measuring bubble populations in gassy marine sediments: a review, In *The Institute of Acoustics Spring Conference-Futures in Acoustics*, TG Leighton, **28**(1), pp. 60-68, 2006.

[16] **PA Hwang, RA Roy** and **LA Crum**, Artificial bubble cloud targets for underwater acoustic remote sensing, *J. Atmos. & Oceanic Tech.*, **12**, pp. 1287-1302, 1995.

[17] **E Silberman**, Sound velocity and attenuation in bubbly mixtures measured in standing wave tubes, *J. Acous. Soc. of Am.,* **29**(8), pp. 925-933, 1957.

[18] **K Hyun, SH Kim, KH Ahn** and **SJ Lee**, Large amplitude oscillatory shear as a way to classify the complex fluids, *J. Non-Newtonian Fluid Mech.*, **107**, pp. 51-65, 2002.

[19] **EL Hamilton**, Elastic properties of marine sediments, *J. Geophys. Res.,* **76**(2), pp. 579-603, 1971

[20] **W Sachse and Y-H Pao,** On the determination of phase and group velocities of dispersive waves in solids, *J. Appl. Phys.*, **49**(8), pp. 4320-4327, 1978.